241th Colloque GANIL, 2026

Microscopic Description of Fragment Angular momentum generation in fission

Guillaume SCAMPS

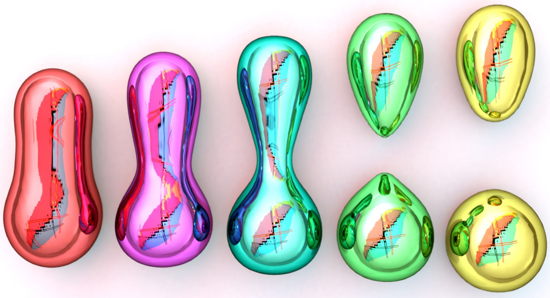

Université de Toulouse

L2IT

cnrs

J. Phys. G: Nucl. Part. Phys. **47** (2020) 113002 Topical Review

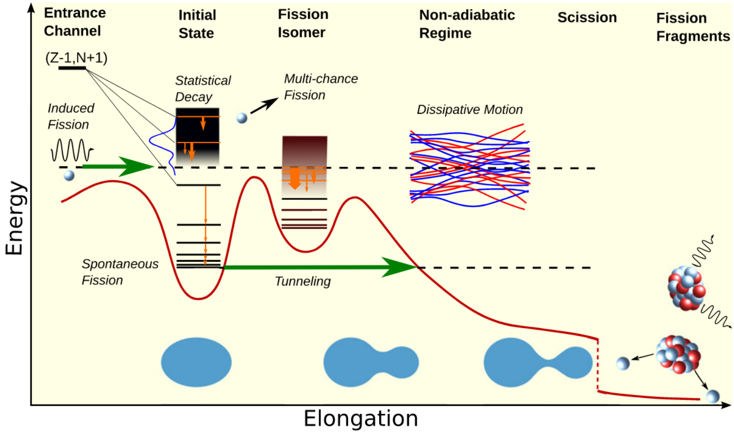

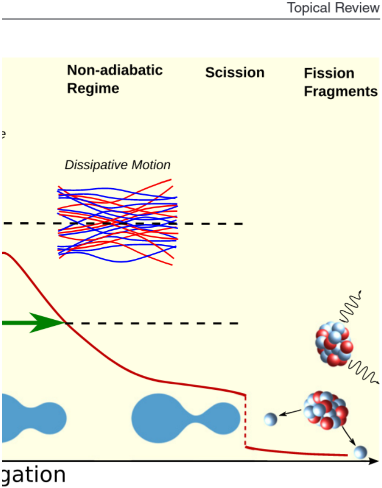
Topical Review
Non-adiabatic Regime
Scission
Fission Fragments
Dissipative Motion
gation

What do we want to understand ?

- Charge and mass distribution
- Connection with structure
- Odd-even effects
- Charge polarization
- Spin-Parity of the fragments

$\rightarrow P(N, Z, J^{\pi}, E^{*})$

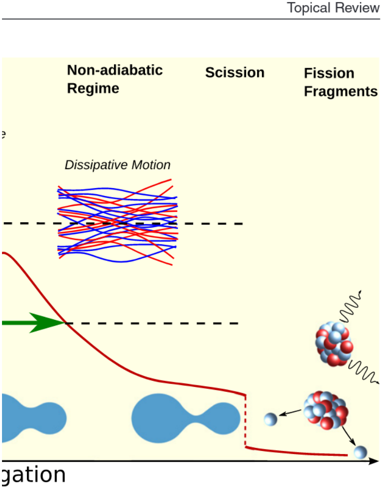

Spin of the fragments

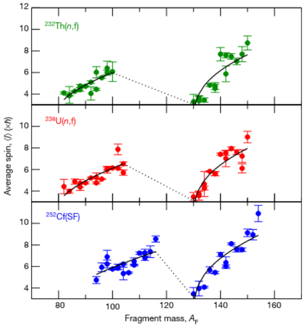

Correlations

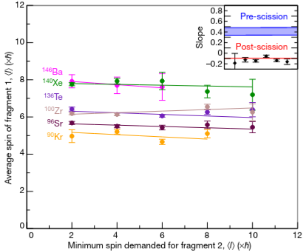

J. N. Wilson, Nature, 590, 566 (2021)

- The average spin follows a sawtooth shape
- No correlations between the spins of the fragments

TDHFB equations

$$i\hbar\frac{\partial}{\partial t}\begin{pmatrix} U \\ V \end{pmatrix} = \begin{pmatrix} h(t) & \Delta(t) \\ -\Delta^*(t) & -h^*(t) \end{pmatrix}\begin{pmatrix} U \\ V \end{pmatrix}$$

TDHFB equations

$$i\hbar\frac{\partial}{\partial t}\begin{pmatrix}U\\V\end{pmatrix}=\begin{pmatrix}h(t) & \Delta(t)\\-\Delta^*(t) & -h^*(t)\end{pmatrix}\begin{pmatrix}U\\V\end{pmatrix}$$

Strengths

- Self-consistent mean field + pairing
- Functional and no other adjustable parameters.
- One-body dissipation
- Large-amplitude collective motion

TDHFB equations

$$i\hbar\frac{\partial}{\partial t}\begin{pmatrix}U\\V\end{pmatrix}=\begin{pmatrix}h(t) & \Delta(t)\\ -\Delta^*(t) & -h^*(t)\end{pmatrix}\begin{pmatrix}U\\V\end{pmatrix}$$

Strengths

- Self-consistent mean field + pairing
- Functional and no other adjustable parameters.
- One-body dissipation
- Large-amplitude collective motion

Limitations

- Missing quantum and statistic fluctuations
- Broken symmetries (projection needed)
- Computationally expensive

First : static PES

Example : ^{240}Pu

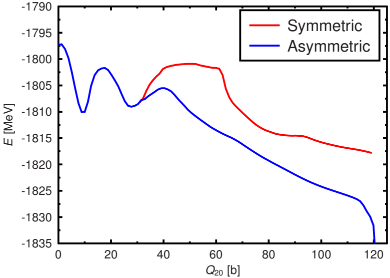

Second : Dynamic

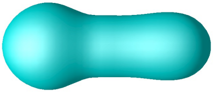

First : static PES

Example : ^{240}Pu

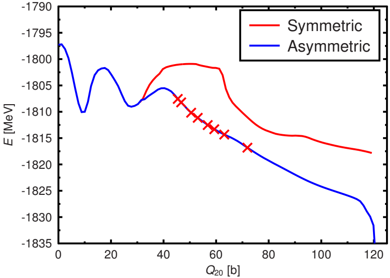

Second : Dynamic

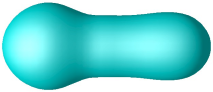

First : static PES

Example : ^{240}Pu

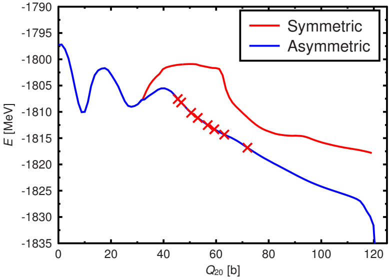

Second : Dynamic

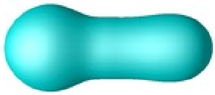

First : static PES

Example : ^{240}Pu

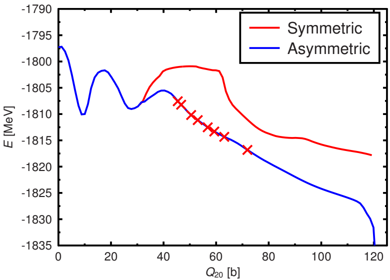

Second : Dynamic

Third : Characterisation of the fragments

Final state :

$$|\Psi\rangle = \prod_k \left(u_k + v_k a_k^\dagger a_{\bar{k}}^\dagger \right) |-\rangle$$

Easy to get the average properties. Difficult to get the distribution

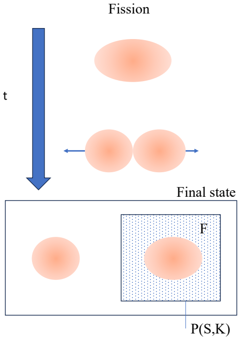

Projection method $\simeq$ theoretical detector

The projector acts as a theoretical detector on the wave function. The probability of measuring $\hat{O} = o$ is

$$P(o) = \langle \Psi | \hat{P}_{\hat{O}=o} | \Psi \rangle$$

Projection on the spin and K number (Projection of the spin on the fission axis)

$$\hat{P}^S_{MK} = \frac{(2S+1)}{16\pi^2} \int d\Omega \mathcal{D}^{S*}_{MK}(\Omega)\, e^{i\alpha \hat{S}_z} e^{i\beta \hat{S}_y} e^{i\gamma \hat{S}_z},$$

$$P(S_F, K_F) = \langle \Psi | \hat{P}^{S_F}_{K_F K_F} | \Psi \rangle,$$

Calculation of the overlap with Pfaffian : G. F. Bertsch and L. M. Robledo, PRL 108, 042505 (2012)

Spin distribution in the fragments

Obtained using 3-angle projection operator

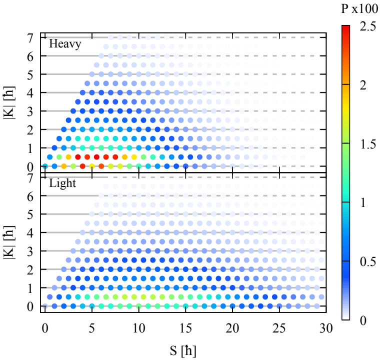

Geometry of the reaction

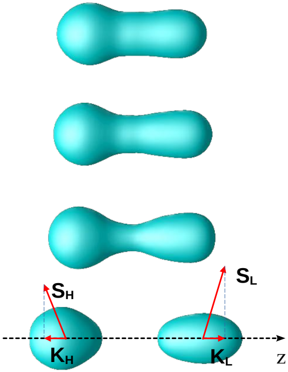

G.scamps, I. Abdurrahman, M. Kafker, A. Bulgac, and I. Stetcu, PRC 108 (6), L061602

Pair breaking mechanism ?

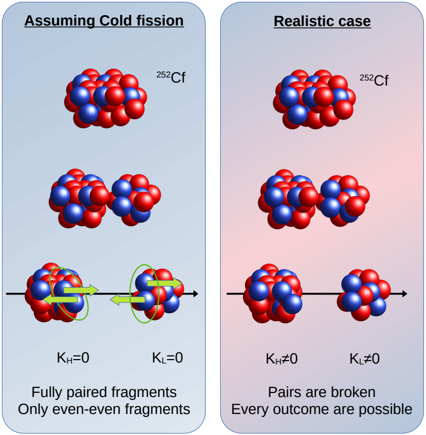

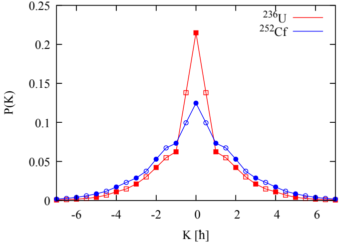

G.scamps, I. Abdurrahman, M. Kafker, A. Bulgac, and I. Stetcu, PRC 108 (6), L061602.

Spins are mostly perpendicular to the fission axis

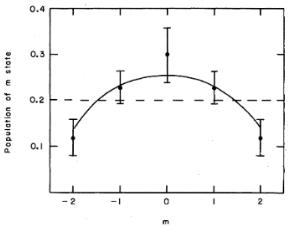

FIG. 9. The points are the calculated populations of the various m substates of the 2^+ level in ^{144}Ba. These values were determined using the fitted experimental angular distribution of the $2^+ \rightarrow 0^+$ γ ray. The solid line represents the predicted population of the m states as calculated from the statistical-model analysis of the de-excitation process using Eqs. (4) and (5) with an assumed value of $B=6$ [Eq. (3)] for the initial angular momentum distribution.

J. B. Wilhelmy, E. Cheifetz, R. C. Jared, S. G. Thompson, H. R. Bowman, and J. O. Rasmussen Phys. Rev. C 5, 2041 (1972)

Uncertainty principle in TDDFT

Can we understand the generation of spin in TDDFT with the uncertainty principle ?

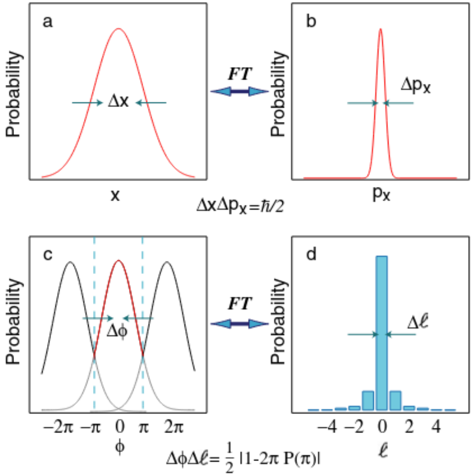

S. Franke-Arnold, et al. New Journal of Physics 6, 103 (2004)

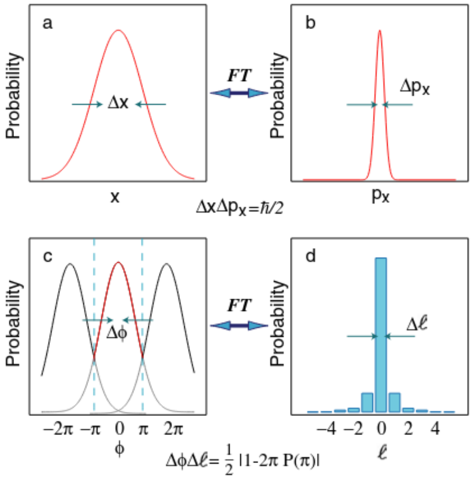

S. Franke-Arnold, et al. New Journal of Physics 6, 103 (2004)

Orientation pumping mechanism

Isotropic potential at scission

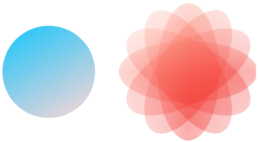

Confining potential at scission

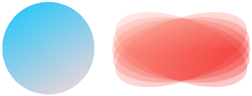

L. Bonneau, P. Quentin, and I. N. Mikhailov, PRC 75, 064313 (2007).

For $\Delta\Theta = 1^\circ$, $\Delta L = 29\hbar$.

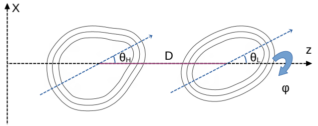

Potential as a function of the light fragment angle

$^{132}Sn + ^{108}Ru$

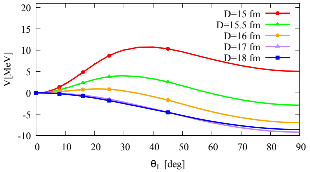

Two torques :

- attractive nucleus-nucleus torque
- repulsive Coulomb torque

Potential as a function of the light fragment angle

$^{144}Ba + ^{96}Sr$. D=15.5 and 20 fm

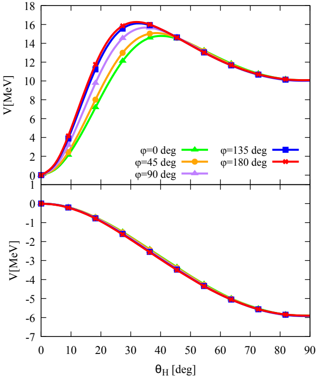

The azimuthal angle doesn't have an important role.

G. Scamps, G. Bertsch, Phys. Rev. C 108, 034616 (2023).

TDHFB framework

- Gogny-TDHFB code
- Gogny D1S interaction
- Hybrid basis :
  - 2D harmonic oscillator (x, y)
  - 1D spatial mesh (z)

Fissioning nuclei

- ^{230}Th
- ^{240}Pu
- ^{250}Cf

Asymmetric fission region
Heavy fragment influenced by octupole deformation

Y. Hashimoto, Time-dependent hartree-fock-bogoliubov calculations using a lagrange mesh with the gogny interaction, PRC 88, 034307 (2013).

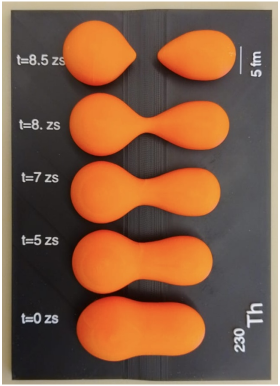

Orientation–Angular Momentum Uncertainty

Conceptual difficulty

- Unlike position, angular variables are **periodic**.
- Mean values and fluctuations of an angle are not uniquely defined.
- Restrict to well-oriented wave packet

Orientation–angular momentum uncertainty

$$\Delta\theta \, \Delta L_x > \frac{1}{2}, \qquad (L_x \text{ in units of } \hbar)$$

Analogous relation for L_y.

Gaussian orientation state and spin distribution

Gaussian wave packet :

$$\Psi(\theta, \varphi) = \mathcal{N} \exp\left[-\frac{\theta^2}{4\sigma_\theta^2}\right]$$

Spin cut-off distribution :

$$P(L) = \frac{2L+1}{\mathcal{Z}} \exp\left[-\frac{L(L+1)}{2\sigma_L^2}\right]$$

Heisenberg-type relation :

$$\sigma_\theta \, \sigma_L = \frac{1}{2}$$

Principal axis determination

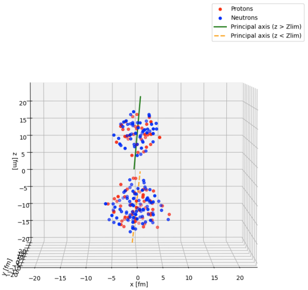

Examples for ^{230}Th.
Red/blue dots : proton/neutron distributions.
Lines : fragment principal axes.

Angular distribution figure

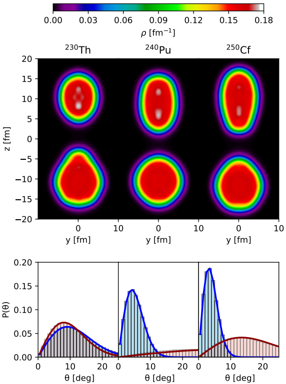

Angular distribution $P(\theta)$ for light (blue) and heavy (red) fragments. Fitted curves illustrate approximate Gaussian behavior.

Nucleoscope paper : A. Bernard *et al.*, Eur. Phys. J. A 62, 112 (2026)

Principal axis determination

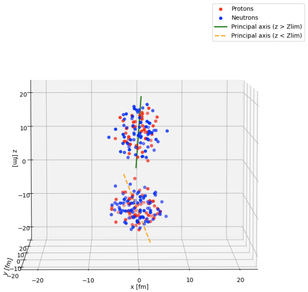

Examples for ^{230}Th.
Red/blue dots : proton/neutron distributions.
Lines : fragment principal axes.

Angular distribution figure

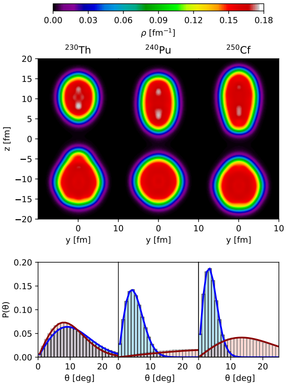

Angular distribution $P(\theta)$ for light (blue) and heavy (red) fragments. Fitted curves illustrate approximate Gaussian behavior.

Nucleoscope paper : A. Bernard *et al.*, Eur. Phys. J. A 62, 112 (2026)

Overlap of rotated many-body states

$$\langle \Psi | e^{i\alpha \hat{J}_z} e^{i\theta \hat{J}_y} e^{i\gamma \hat{J}_z} | \Psi \rangle \simeq \exp\left[-\frac{\theta^2}{8\sigma_\theta^2} \right]$$

- Gaussian approximation for small rotations
- Width σ_θ characterizes angular localization

Physical meaning

- Many-body state localized in rotational space
- Does **not** rely on geometric definition of orientation
- Orientation angle and angular momentum are conjugate variables

Spin fluctuations

Spin cut-off distribution :

$$P(J) = \frac{2J+1}{\mathcal{Z}} \exp\left[-\frac{J(J+1)}{2\sigma_J^2} \right]$$

$$\sigma_\theta \, \sigma_J = \frac{1}{2}$$

Nucleus	Frag.	σ_L (uncert. with principal axis)	σ_J (uncert. with overlap)	σ_J (projection)
^{230}Th	L	2.90	5.74	5.81
	H	3.37	7.84	7.88
^{240}Pu	L	6.79	9.32	9.37
	H	0.75	4.67	4.93
^{250}Cf	L	9.00	12.18	12.27
	H	2.12	6.50	6.63

Key result

- Spin cut-off parameters extracted from :
  - angular fluctuations + uncertainty relation
  - Gaussian overlap fit
  - exact angular-momentum projection
- **very good agreement** between overlap and exact projection.
- Error with the principal axis method (miss higher order deformation).

G. Scamps, A. Guilleux, D. Regnier, A. Bernard, Uncertainty Principle and Angular Momentum Generation in Microscopic Fission Models, arXiv :2512.02207 [nucl-th].

Spin-parity distribution

Fission as a quantum transition

$$(J_0, \pi_0) \rightarrow (J_1, \pi_1) + (J_2, \pi_2) + L$$

$$\boldsymbol{J}_0 = \boldsymbol{J}_1 + \boldsymbol{J}_2 + \boldsymbol{L}$$

$$\pi_0 = \pi_1 \pi_2 (-1)^L$$

Conservation rules are not constraining

State-of-the-art models of fragment decay assume a simple, equiprobable partition between positive and negative parities

Fragment parity projection

$$\hat{P}_F^{\pi} = \frac{1}{2}(1 + \pi \hat{\Pi}_F)$$

$$P_F(J, K, \pi, N, Z) = \langle \Psi | \hat{P}_F^N \hat{P}_F^Z \hat{P}_{KK,F}^J \hat{P}_F^{\pi} | \Psi \rangle$$

Fragment quantum numbers obtained by simultaneous projections

+ comparison Skyrme Skm* (P. Marević, A. Bjelčić, N. Schunck) - Gogny D1S

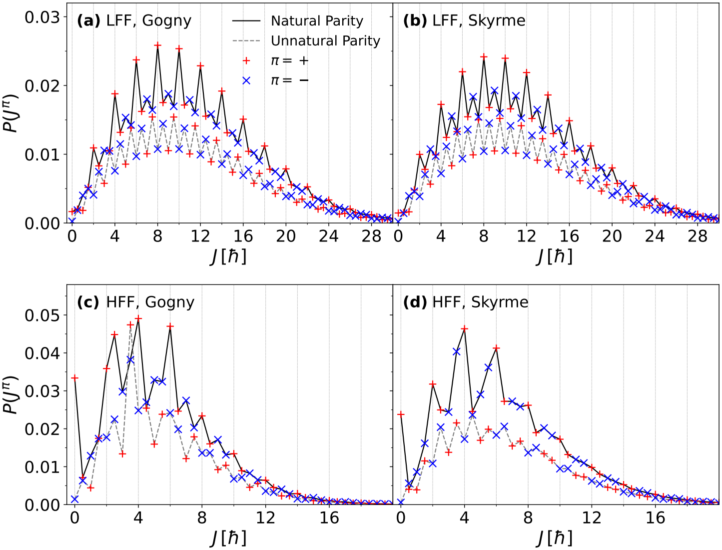

G. Scamps, P. Marević, A. Bjelčić, N. Schunck, *Microscopic Spin-Parity Distributions of Fission Fragments*, arXiv :2607.24156 [nucl-th]

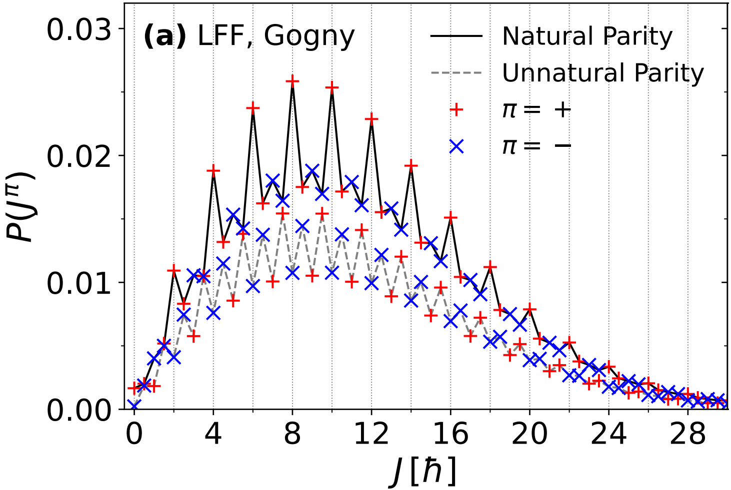

G. Scamps, P. Marević, A. Bjelčić, N. Schunck, *Microscopic Spin-Parity Distributions of Fission Fragments*, arXiv :2607.24156 [nucl-th]

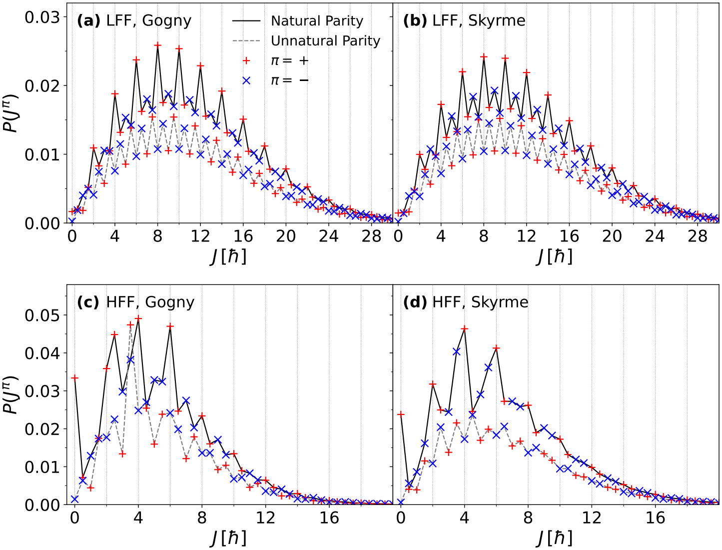

G. Scamps, P. Marević, A. Bjelčić, N. Schunck, *Microscopic Spin-Parity Distributions of Fission Fragments*, arXiv :2607.24156 [nucl-th]

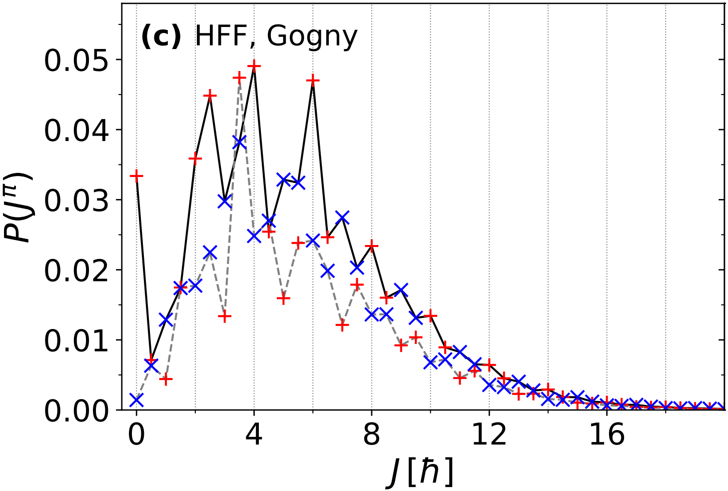

G. Scamps, P. Marević, A. Bjelčić, N. Schunck, *Microscopic Spin-Parity Distributions of Fission Fragments*, arXiv :2607.24156 [nucl-th]

Nuclear structure	Symmetry	Allowed spins	Parity pattern
Spherical even-even	Full rotational symmetry	$J = 0$ and $K = 0$	0^+
Quadrupole-deformed	Axial symmetry + reflection	$J = 0, 2, 4, \ldots$ and $K = 0$	$\pi = +$ (natural)
Octupole-deformed	Broken reflection symmetry	$J = 0, 1, 2, 3, \ldots$ and $K = 0$	Alternating $\pi = (-1)^J$ (natural)
Pair breaking (q.p. excitation)	Broken pairing symmetry	All J and K accessible	Natural + unnatural

$\boxed{\text{Symmetry breaking} \longrightarrow \text{characteristic spin–parity signatures}}$

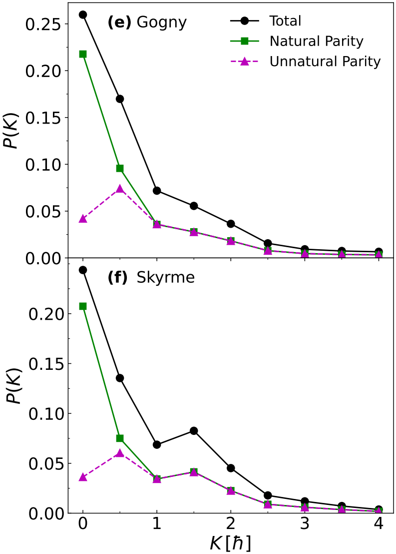

G. Scamps, P Marević, A. Bjelčić, N. Schunck, Microscopic Spin-Parity Distributions of Fission Fragments, arXiv :2607.24156 [nucl-th]

Light fragment spin–parity

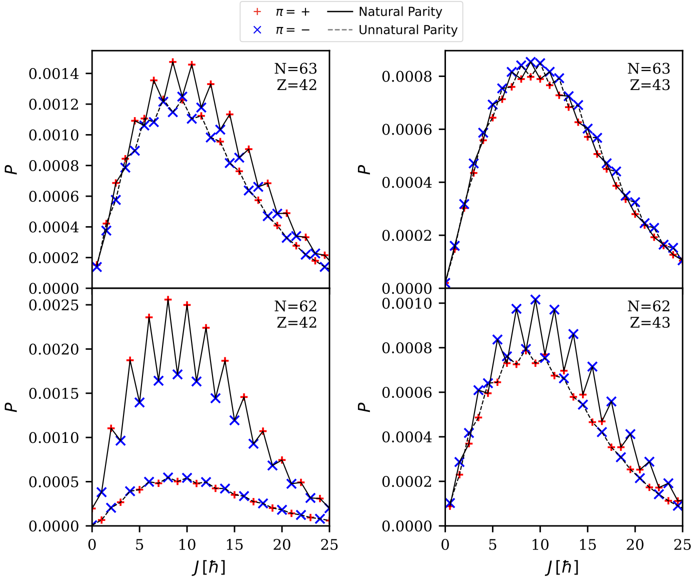

Light fragment spin–parity

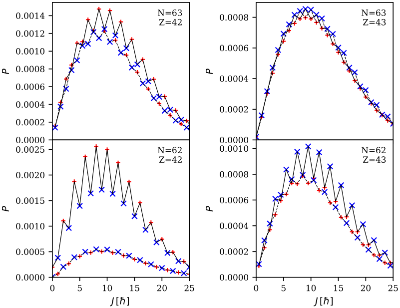

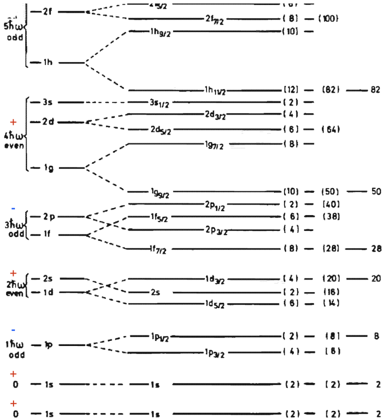

Ring and Schuck, The Nuclear Many-Body Problem

Heavy fragment spin–parity

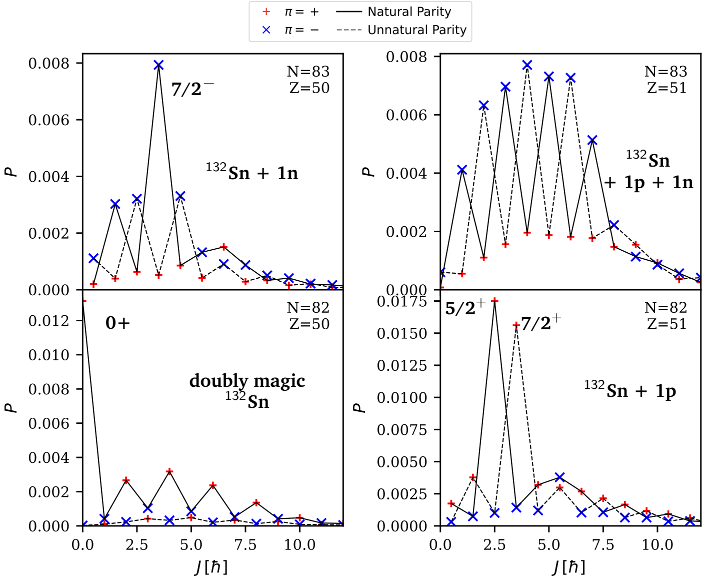

Heavy fragment spin–parity

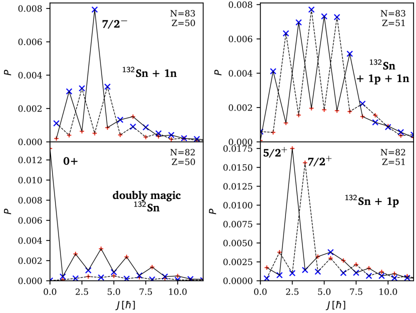

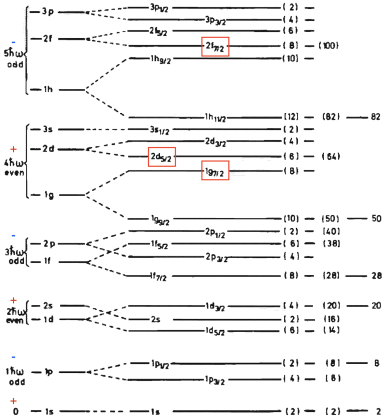

Ring and Schuck, The Nuclear Many-Body Problem

Parity as a function of the mass

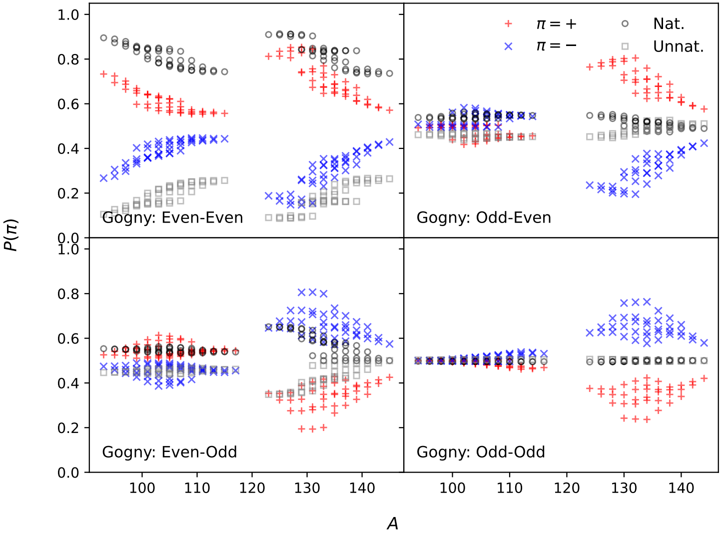

G. Scamps, P Marević, A. Bjelčić, N. Schunck, Microscopic Spin-Parity Distributions of Fission Fragments, arXiv :2607.24156 [nucl-th]

- **Complete spin–parity characterization**

$$P(J, K, \pi, N, Z)$$

of fission fragments obtained with projection operators using Gogny D1S and Skyrme SkM* EDFs.

- **Origin of fragment angular momentum**
  - Light fragments : dominated by collective quantum fluctuation.
  - Heavy fragments : microscopic structure and single-particle effects become important.

Pair breaking effects

- Population of odd Z
- Generates non-zero K components.
- Explains unnatural-parity configurations.

- **Impact for fission observables**
  - Current de-excitation models assume random equal parity.
  - Including parity distributions may modify simulated observables.

Thank you for your attention

Thanks to my collaborators : George Bertsch, Alice Bernard, David Regnier, Antoine Guilleux, Aurel Bulgac, Ionel Stetcu, Ibrahim Abdurrahman, Matthew Kafker, Petar Marević, Nicolas Schunck, Antonio Bjelčić, Yukio Hashimoto

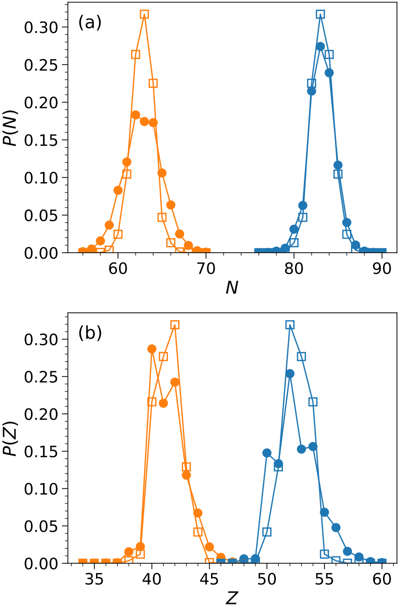

(a)
P(N)
N
0.00
0.05
0.10
0.15
0.20
0.25
0.30
60
70
80
90
(b)
P(Z)
Z
35
40
45
50
55
60

In spontaneous fission of a 0^+ state

$$\mathbf{S_H} + \mathbf{S_L} + \mathbf{\Lambda} = \mathbf{0},$$

Triangular rule :

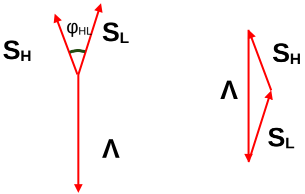

$$\cos(\varphi_{HL}) = \frac{\Lambda(\Lambda+1) - S_H(S_H+1) - S_L(S_L+1)}{2\sqrt{S_H(S_H+1)S_L(S_L+1)}}$$

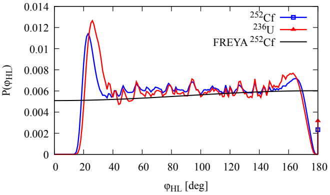

G.Scamps, I. Abdurrahman, M. Kafker, A. Bulgac, and I. Stetcu, PRC 108 (6), L061602.

One angle projector :

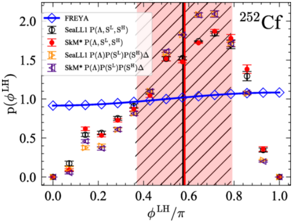

Non alignement of the spins

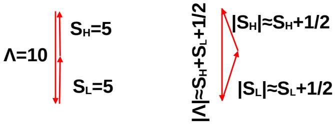

To get a 5 degrees angle between two spins require spins of 262 $\hbar$ and 6565 $\hbar$ for 1 degree

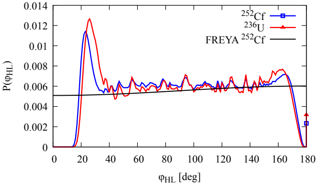

Evolution of a three-angle wave packet

Correlation between the angular momentum

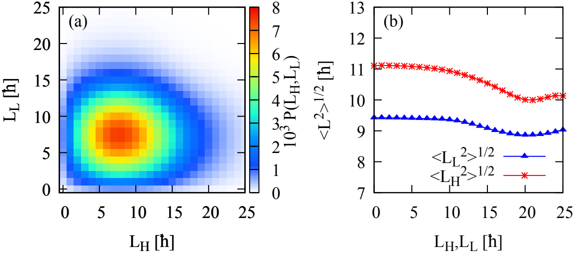

^{144}Ba+^{96}Sr

- No or small correlation observed in the magnitude of the angular momentum.
- More angular momentum for the heavy fragment

Effect of octupole deformation

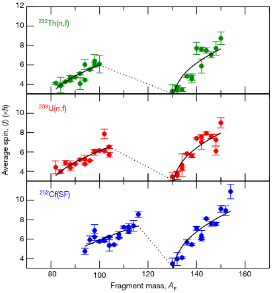

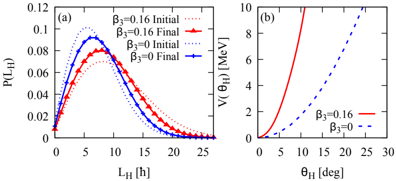

G. Scamps, G. Bertsch, Phys. Rev. C 108, 034616 (2023).

Mechanism

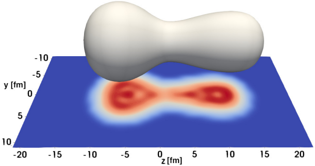

- Pear-shaped deformation plays an important role at scission. G. Scamps C. Simenel, Nature 564, pages 382–385 (2018)
- Octupole deformation makes the angular potential stiffer which increase the zero-point motion $\rightarrow$ more angular momentum

Orbital angular momemtum

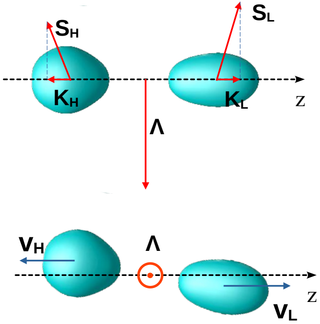

In spontaneous fission of a 0^+ state

$$\mathbf{S_H} + \mathbf{S_L} + \mathbf{\Lambda} = \mathbf{0},$$

Triangular rule :

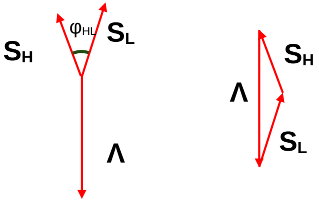

$$\cos(\varphi_{HL}) = \left(\frac{\Lambda(\Lambda+1) - S_H(S_H+1) - S_L(S_L+1)}{2\sqrt{S_H(S_H+1)S_L(S_L+1)}} \right)$$

Evolution of a three-angle wave packet

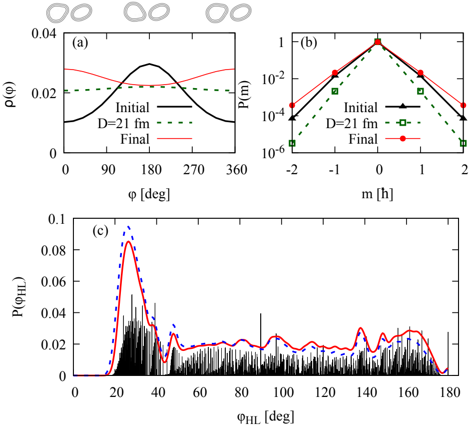

G. Scamps, G. Bertsch, Phys. Rev. C 108, 034616 (2023).

Geometry

- Small azimuthal correlation
- Spins are perpendicular to the fission axis
- Complex pattern in the opening angle, different from previous model

Vanishing pairing during dynamics ?

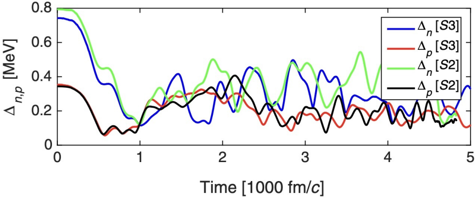

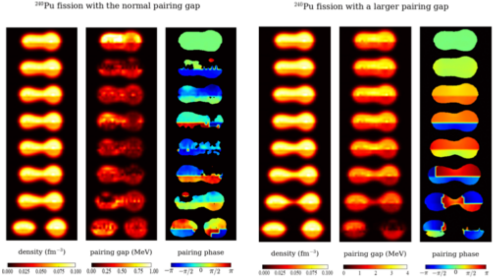

A. Bulgac, P. Magierski, Kenneth J. Roche, and I. Stetcu, PRL 116, 122504 (2016).
A. Bulgac, S. Jin, K. J. Roche, N. Schunck, and I. Stetcu, PRC 100, 034615 (2019).